Moroccan Journal of Chemistry
ISSN: 2351-812X
http://revues.imist.ma/?journal=morjchem&page=login
Kaour & al. / Mor. J. Chem. 9 N°4 (2021) 715-727
DOI: https://doi.org/10.48317/IMIST.PRSM/morjchem-v9i3.26577

Removal of Eriochrome Black T dye from aqueous solutions by using nano-crystalline calcium phosphate tricalcic apatitic

J.Kouar[(a,b)*], T.Ould Bellahcen[(c)], A.El Amrani [(d)], A.Cherif [(e)], N.Kamil [(f)]

[(a)] Department of Chemistry and Valorization (CV), Faculty of Sciences Aïn Chock of Casablanca, Hassan II University of Casablanca, Morocco

[(b)] Laboratory of Process Engineering and Environment (LIPE), High School of Technology of Casablanca, Hassan II University of Casablanca, Morocco

[(c)] Laboratory Health and Environment, Faculty of Science Aïn Chock of Casablanca, Hassan II University of Casablanca, Morocco

[(d)] Laboratory Synthesis, Extraction and Physico-Chemical Study of Organic Molecules, Faculty of Sciences Aïn Chock of Casablanca, Hassan II University of Casablanca, Morocco

[(e)] Laboratory of Materials Engineering for Environment and Valorisation (GEMEV), Faculty of Sciences Aïn Chock of Casablanca, Hassan II University of Casablanca, Morocco

[(f)] Laboratory of Production Mechanics and Industrial Engineering (LMPGI), High School of Technology of Casablanca, Hassan II University of Casablanca, Morocco

** Corresponding author:*
Kouarjihane@gmail.com

Received 01 Jun 2021
Revised 05 Dec 2021;
Accepted 06 Dec 2021

Abstract

Calcium phosphate tricalcic apatitic (CaPT-Ap) was synthesized by co-precipitation at low temperature and basic medium. The potential of CaPT-Ap as an adsorbent was investigated in a batch reactor under different experimental conditions for removing dye Eriochrome Black T (EBT) from aqueous solutions. The used adsorbent was characterized by X-ray diffraction (XRD), infrared spectroscopy (FTIR) and chemical analysis indicate that this calcium phosphate is a CaPT-Ap. The effect of particle sizes , mass of the adsorbent, contact time ,temperature and the concentration of the dye on the adsorption were determined. The kinetic study showed that the pseudo-second-order model gives a better description of the kinetics of the adsorption reaction than the pseudo-first-order model. Analysis of adsorption isotherms showed that adsorption governed by the isotherms of Freundlich. Thermodynamic parameters such as ΔG°, ΔS° and ΔH° were calculated. It was found that EBT dye adsorption was spontaneous and endothermic.

Keywords: *Adsorption; kinetic; Isotherms; calcium phosphate tricalcic apatitic (CaPT-Ap); Eriochrome Black T (EBT); decolourization.*

1. Introduction

The world has seen a raw development in technology to meet the needs of the world, especially in the textile field with the increase of demand for textiles which in turn increases the demand for textile dyes. This pushes us to make the treatment of wastewater our environmental priority. Adsorption techniques are widely used to remove dyes from wastewater [1]–[3]. It is currently known that a great part of natural calcium phosphates adopts a crystalline structure similar to that of synthetic hydroxyapatite $Ca_{10}(PO_4)_6(OH)_2$ [4]–[8] The composition of natural phosphates is very complex. Indeed, the lattice allows various anionic and cationic substitutions [5], [9]–[12]. Despite their low cost and their availability in the market, the use and application of apatite as adsorbents is still a subject of relatively scarce investigations, chromium [13] nickel [14] dyes [15] industrial gas [16] Proteins [17] fluoride[18]–[21] phenolic substances [22] pharmaceutical contaminant [23]. In addition, several studies have shown that this material can be efficient matrices of water purification [20][24]. However, as far as we know, it is the first time that in the present work, we studied the use of calcium phosphate tricalcic apatitic (CaPT-Ap) prepared by co-precipitation at ambient temperature and basic medium as adsorbent to remove dye Eriochrome Black T (EBT) in aqueous solution. The synthesized CaPT-Ap was characterized using several experimental techniques such as X-ray diffraction, FT-IR spectroscopy and chemical analysis.

2. Materials and methods

2.1. Materials

2.1.1. Synthesis and Characterization of the adsorbent material

The adsorption tests were conducted on a calcium phosphate: calcium phosphate tricalcic apatitic (CaPT-Ap) $Ca_9(PO_4)_5(HPO_4)(OH)$ [25]. Its powder was prepared at room temperature by an aqueous double decomposition method of the salts of calcium and phosphate [26]; so to have nanoparticles and a large area, the solution A was quickly poured at room temperature [27] into a stirred reactor containing the solution B, stirring quickly for a few minutes and the precipitate was filtered under vacuum pump on a Buchner's funnel, washed with distilled water containing ammonia and finally dried in the oven at 120°C for 24 h. The adsorbent is crushed and sieved to obtain different particle sizes. The solution A: to 47 g of calcium nitrate $Ca(NO_3)_2{\cdot}4H_2O$ (Reidel-de haen,97%) prepared in 550 ml of distilled water, 20 ml of ammonia solution(d = 0.91) was added. The solution B: to 26 g of di-ammonium hydrogen phosphate $(NH_4)_2HPO_4$ (Reidel-de haen 99%) prepared in 1300 ml of distilled water, 20 ml ammonia solution (d = 0.91) was added. The calcium and the phosphate ion content in the powder were determined respectively by complexometry with EDTA and by spectrophotometry after the formation of the blue phosphomolybdate complex (λ_{max} = 880 nm). The constitution and phase purity of the synthesized powders were checked by X-ray diffractometry using a Bruker D8 Advance apparatus. The presence of functional groups was also investigated by the Fourier transform infrared (FTIR) spectroscopy. A mixture of synthesized powder and spectroscopic grade KBr was ground in an agate mortar and was pressed to obtain a thin transparent pellet. IR spectra were collected by a Shimadzu IR Affinity-1S FTIR spectrometer in the spectral range 4000-400 cm^{-1}.

2.1.2. Adsorbate

The physical characteristics of Eriochrome Black T (EBT) which is an acidic synthetic dye are given in ***Table 1***. It was provided by "Labochemie".

Table 1. ***Characteristics of Eriochrome Black T***

Molecular structure	Formula	Molar mass ($g.mol^{-1}$)	Index color	λ_{max} (nm)	Nature/ type
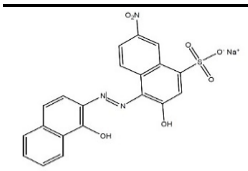	$C_{20}H_{12}N_3NaO_7S$	461.38	C.I 14645	530	Azo/ anionic dye

2.2. Adsorption experiment

In this part, we have studied the effect of dyes concentrations, mass of adsorbent, duration time and the particle sizes on the adsorption of EBT by CaPT-Ap. The batch adsorption experiments were carried out at ambient temperature in conical flasks at a constant agitation speed of 500 rpm by varying the adsorbent dosage from 0 to 4.0 $g.L^{-1}$; the duration time is about 4h; the initial dyes concentrations were from 5 to 100 $mg.L^{-1}$, the particle sizes were from 0 to1mm and the temperature range 7 to 60°C. The pH was about 6.10. Different amount of CaPT-Ap nanoparticles was added to EBT solution (previously known concentration); the mixing operation was done for adsorption in multiple shakers. After each adsorption experiment, the samples were centrifuged at 4000 rpm for 10 min to separate the solid phase from the liquid one. The supernatants were analyzed for residual dye concentrations by a T60 UV/Vis spectrophotometer. The quantity of dye adsorbed and percentage removal were calculated by the following expressions (1) and (2):

$$\%Removal=\frac{(C_0-C_e)}{C_0}\times 100 \quad (1)$$

$$q_e=\frac{(C_0-C_e)}{m}V \quad (2)$$

were the *m* is the mass of adsorbent (g), V the volume of the solution (L),C_0 the initial concentration of adsorbate ($mg.L^{-1}$), C_e is the equilibrium adsorbate concentration ($mg.L^{-1}$), and q_e is the amount of adsorbate adsorbed per unit mass of adsorbent ($mol.g^{-1}$) at equilibrium (mg of EBT per g of adsorbent CaPT-Ap) .

2.3. Kinetic study

The contact time is one of the important parameters for the successful application of adsorption procedures to understand in details the exact dynamics mechanism of the adsorption process, three general kinetics models, namely, pseudo-first-order, pseudo-second-order and second-order were applied to the experimental data [28].

The linear forms of these models are given in equation (3), (4) and (5) respectively:

Pseudo first order equation:

$$Log_{10}(q_e-q_t)=\log q_e-\frac{k_1}{2{,}303}t \quad (3)$$

Pseudo second order equation:

$$\frac{t}{q_t}=\frac{1}{k_2 q_e^2}+\frac{1}{q_e}t \quad (4)$$

Second order equation:

$$\frac{1}{(q_e-q_t)}=\frac{1}{q_e}+k_3 t \quad (5)$$

Where; q_t and q_e are the adsorption capacities at time t and equilibrium, respectively ($mg.g^{-1}$), t is the contact time (min). k_1 is the rate constant of pseudo-first-order adsorption (min^{-1}), k_2 is the rate constant of pseudo-second-order adsorption ($g\ min^{-1}\ mg^{-1}$) and k_3 is the rate constant of second-order adsorption ($g\ min^{-1}\ mg^{-1}$).

To plot log (q_e-q_t) versus t gives a linear relationship from which k_1 and q_e can be determined from the slope.

The plot of t/q_t versus t shows a linear relationship and allows us to calculate k_2 and q_e. From the plot of $1/(q_e-q_t)$ versus t, we can calculate k_3 and q_e.

2.4. Adsorption Isotherm

Experimental data were simulated with linear forms of Langmuir [29] and Freundlich [30] models, recommended for dye adsorption. The linearized form of Langmuir (6) and Freundlich (7) equations are expressed as follows:

$$\frac{C_e}{q_e} = \frac{1}{q_{max}} C_e + \frac{1}{q_{max} K_L} \quad (6)$$

$$\text{Log } q_e = \log K_F + \frac{1}{n} \log C_e \quad (7)$$

Where q_e is the amount of BET adsorbed per unit mass of adsorbent ($mg.g^{-1}$); C_e is the equilibrium concentration of BET solution ($mg.L^{-1}$); q_{max} the maximum quantity adsorbed. The constants K_F, K_L and n of the model can be determinate from the slop of the plot of C_e/q_e versus C_e and the plot of log q_e versus log C_e. Langmuir isotherm assumes the homogenous nature of adsorption with equal energy of the entire active adsorption sites [31] and Freundlich isotherm applies to heterogeneous surfaces [32].

2.5. Adsorption thermodynamic:

Temperature is an important factor in the adsorption process and the adsorbent's performance at equilibrium. The adsorption phenomenon is always accompanied by a thermal process which can be either exothermic ($\Delta H° < 0$) or endothermic ($\Delta H° > 0$) and the measurement of the heat of adsorption ΔH is the main criterion that differentiates the process of chemisorption from physisorption. To evaluate the effect of temperature on adsorption process of BET onto the adsorbent powder, thermodynamic parameters such as standard Gibbs free energy change ($\Delta G°$), enthalpy change ($\Delta H°$) and entropy change ($\Delta S°$) are determined according to the equations:

$$\Delta G^0 = -RT\ln K \quad (8)$$

$$K = \frac{q_e}{C_e} \quad (9)$$

$$\ln K = \frac{\Delta S°}{R} - \frac{\Delta H°}{RT} \quad (10)$$

$$\Delta G° = \Delta H° - T\,\Delta S° \quad (11)$$

Were; K is the distribution coefficient, $\Delta G°$ is the Gibbs free energy change **(**$J.mol^{-1}$**),** $\Delta H°$ is the enthalpy change **(**$J.mol^{-1}$), $\Delta S°$ is the entropy change **(**$J.mol^{-1}.K^{-1}$**),** T is the absolute temperature in Kelvin (°K), R is the universal gas constant (8.31 $J.K^{-1}.mol^{-1}$), C_e the equilibrium adsorbate concentration in the aqueous phase ($mg.l^{-1}$),q_e the amount of EBT adsorbed per unit mass of adsorbent ($mg.g^{-1}$) .Plotting the linear transform of Ln (K) versus (1 / T) gives a straight line with slope and intercept equal to $-\Delta H°/R$ and $\Delta S°/R$.This allows us to determinate by identification with the equations, the enthalpy $\Delta H°$ and entropy $\Delta S°$ of adsorption and deduces the Gibbs free energy ΔG ° at different temperatures.

3. Result and discussion

3.1. Characterization of material

3.1.1. FTIR

The IR spectrum of the sample is presented in ***Figure 1***, the bands appearing at 1097 and 1035, 961, 603 and 564 and 471 cm^{-1} are assigned respectively to the ν_3 (P-O) asymmetric stretching mode, ν_1 (P-O) symmetric stretching mode, ν_4 (O-P-O) bending mode and ν_2 (O-P-O) bending mode [33]. Broadbands appearing at around 3446 and 1645 cm^{-1} could be linked to adsorbed water[34]. A sharp peak at 3569 cm^{-1} is associated with OH^- stretching mode and a peak appearing at 632 cm^{-1} is also related to bending mode [35]–[39]. There is also a low-intensity band at 875cm^{-1} which

could be ascribed to the structural HPO_4^{2-} entities [40], [41]. The presence of HPO_4^{2-} and OH^- ions confirms that this calcium phosphate prepared by co-precipitation in the basic medium at ambient temperature is a CaPT-Ap [42] [43]. Our results are following the literature in which the authors reported the same calcium phosphate [13], [15], [44].

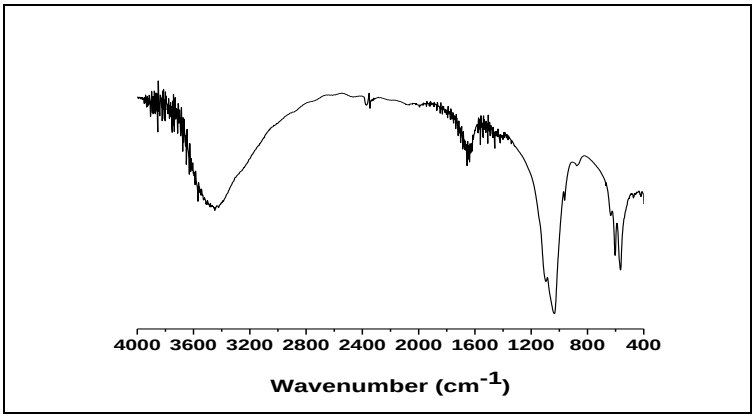

Figure 1. Infrared transmission spectrum of CaPT-Ap

3.1.2. XRD

Figure 2 shows the X-ray diffraction pattern for the dried calcium phosphate. The XRD pattern shows a broad peak indicating that the powder is poorly crystalline and CaPT-Ap, without the presence of impurity phases. Our XRD data were found to be consistent with literature [13], [15], [20], [42], [45].

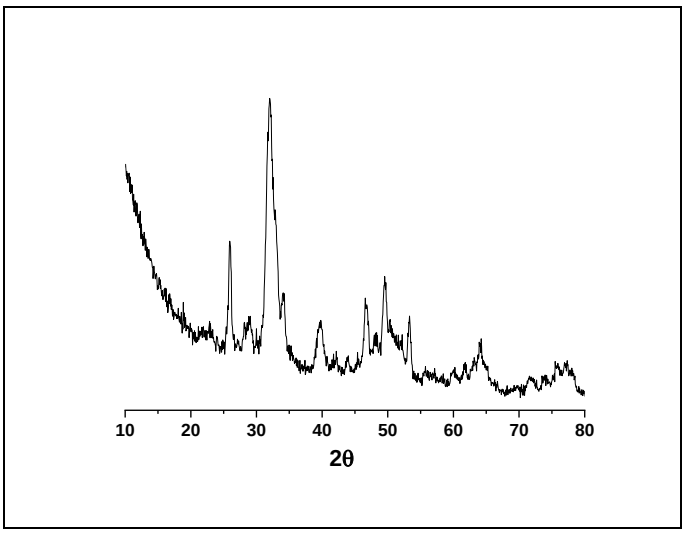

Figure 2. XRD pattern of the dried CaPT-Ap

3.1.3. Chemical analysis

From chemical analysis, our adsorbent was found to have an average Ca/P ratio of 1.49 (28.1 % wt P; 14.6 % wt Ca) which allow us to confirm that this calcium phosphate tricalcic apatitic CaPT-Ap [26][27].

3.2. Adsorption study

3.2.1. Effect of particles size

The effect of adsorbent's particles size was studied in the range of 0-1mm (0-255µm, 255-450µm, 450µm -1mm) for checking the maximum adsorption of EBT at ambient temperature and pH = 6.10. The smallest mesh particles (0-255µm) presents a larger surface area that was shown to be the best for adsorption (***Figure 3***).

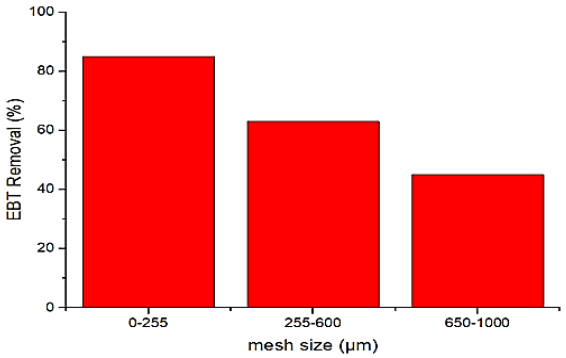

Figure 3. Particles size effect on removal of the EBT

3.2.2. Effect of adsorbent dose

The effect of adsorbent dose was investigated, by varying the mass CaPT-Ap (0-255µm) from 0 to 4 $g.L^{-1}$ which was added to EBT whose initial concentration was 10 $mg.L^{-1}$. The others parameters were kept constants. ***Figure 4*** shows that the efficiency capacity of removal EBT dye increased and reached its maximum (85%) at the addition of adsorbent dose 1$g.L^{-1}$.In addition, the adsorption capacity decreased with the increase of adsorbent dosage. We suggest that these results can be explained that at high doses of adsorbent added, the available sites decreased.

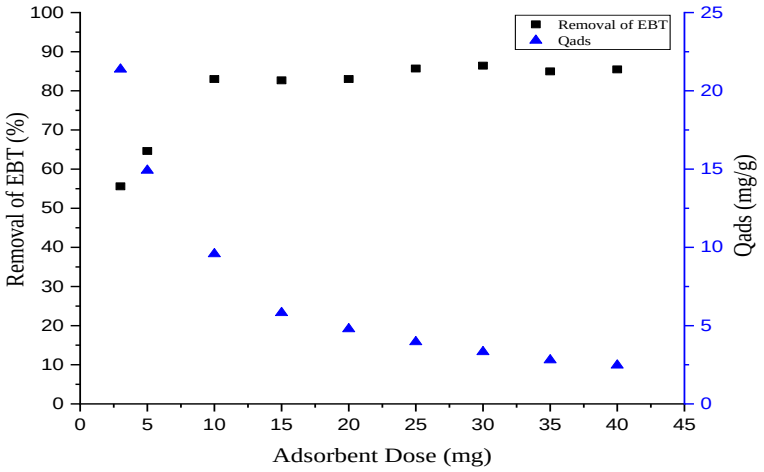

Figure 4. Effect of adsorbent dose on the removal of EBT and the quantity adsorbed

3.2.3. Effect of contact time

Figure 5 presents the effect of contact time on the adsorption of dye on CaPT-Ap. The percentage of removal EBT and the quantity of dye adsorbed per unit mass of adsorbent increase fastly with increasing of contact time and achieved the maximum within the first minutes. Both the maximum adsorption and the removal percentage were respectively 7 $mg.g^{-1}$ and 77.5%. It is found that the evolution of the adsorption rate during the first minutes is very important and it decreases slowly until it becomes zero at the end of the adsorption phenomena.

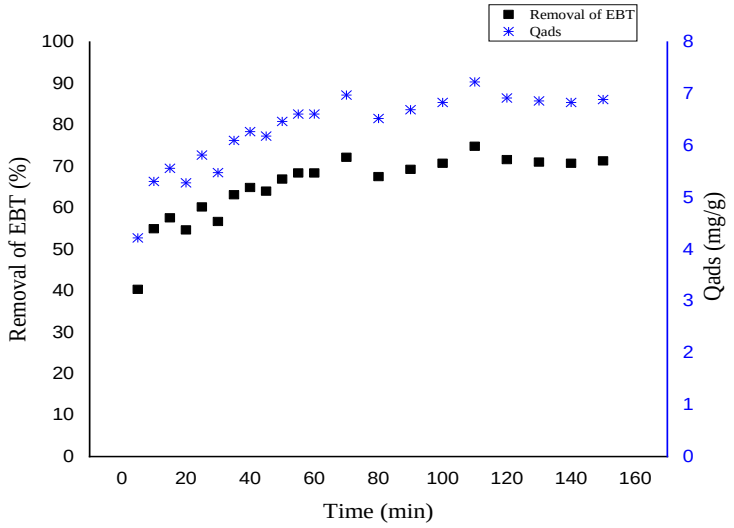

Figure 5. Effect of contact time on the percentage of removal of EBT and the quantity adsorbed of EBT

3.2.4. Effect of initial concentration

Figure 6 shows that the capacity of adsorption decreases from 92% to 74% when the dye concentration increased from 10 to 100 mg.L^{-1}. This result can be explained by the fact that available active sites are insufficient when the initial dye concentration is high.

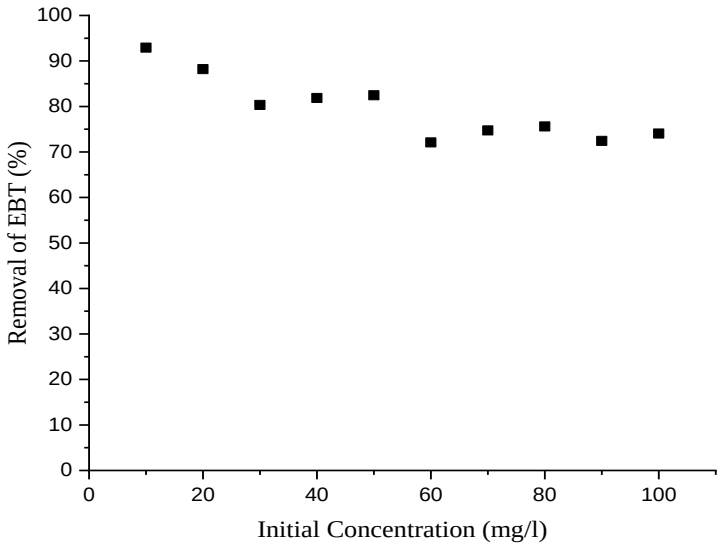

Figure 6. Effect of initial concentration on the removal of EBT

3.2.5. Effect of temperature

Figure 7 illustrates the evolution of the elimination rate as a function of temperature. Note that the rate of elimination increases with increasing temperature and the capacity of adsorption increases with the also increases with temperature. The per cent adsorption of these dyes onto the adsorbent increases from 52 to 65% respectively, with rising in temperature of dye solution from 7 to 60 °C.

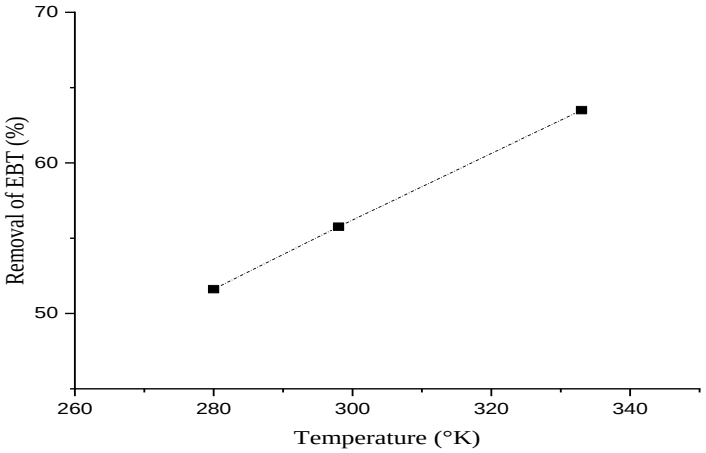

Figure 7. Effect of temperature on removal of EBT

3.3. Kinetic study

Figure* 8** presents the plot of the linear transforms of the three kinetic models. The linear variation of t/qt with the time suggests that the pseudo-second-order model describes well the kinetic behaviour of the EBT adsorption on CaPT-Ap (R^2=0.987). The experimental adsorption $Q_{e,exp}$ (7 $mg.g^{-1}$) is very close to the obtained ($Q_{e,cal}$) by the pseudo-second-order (Table* 2**). According to this latter model, we can state that the adsorption of EBT on CaPT-Ap involves the chemisorption process in addition to the physisorption [46].

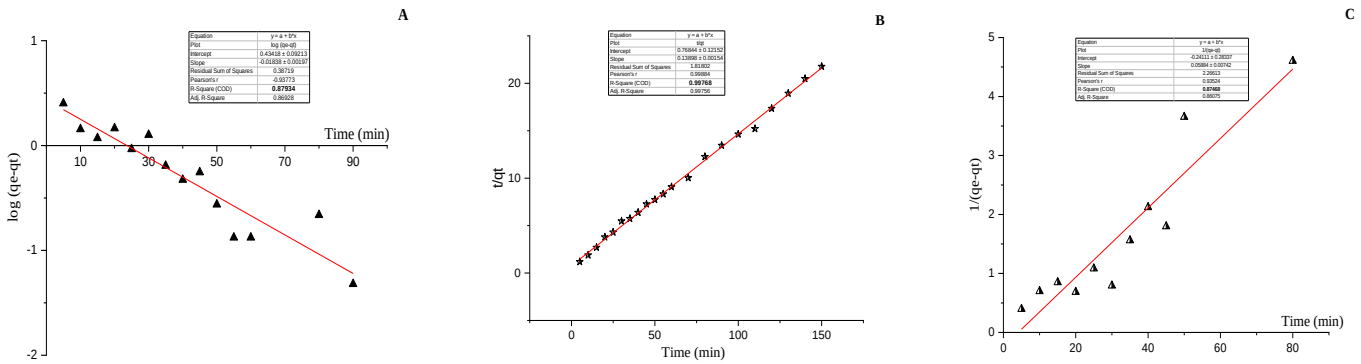

Figure 8. Plots of Pseudo first order (A) Pseudo second-order (B) Second-order (C)

Table 2. ***Kinetics parameters for EBT adsorption by CaPT-Ap***

Experimental	**Pseudo-first-order model**			**Pseudo-second-order model**			**Second-order model**		
$Q_{e,exp}$ ($mg.g^{-1}$)	$Q_{e,cal}$ ($mg.g^{-1}$)	k_1 (min^{-1})	R^2	$Q_{e,cal}$ ($mg.g^{-1}$)	k_2 (min^{-1} $g.mg^{-1}$)	R^2	$Q_{e,cal}$ ($mg.g^{-1}$)	k_3 ($min^{-1}g.mg^{-1}$)	R^2
7	2.59	0.0368	0.801	6.53	0.049	0.987	7.630	0.0398	0.748

3.4. Adsorption isotherms

Figure 9 presents the plot of the linear transforms of the two adsorptions isotherms models Langmuir and Freundlich. The linear variation of Ln(Q_e) versus Ln(C_e) suggests that the Freundlich model fits well the experimental values (R^2 = 0.965) (***Table 3).*** According to this later model, we can conclude that the EBT adsorption by CaPT-Ap is done on a heterogeneous surface [32].

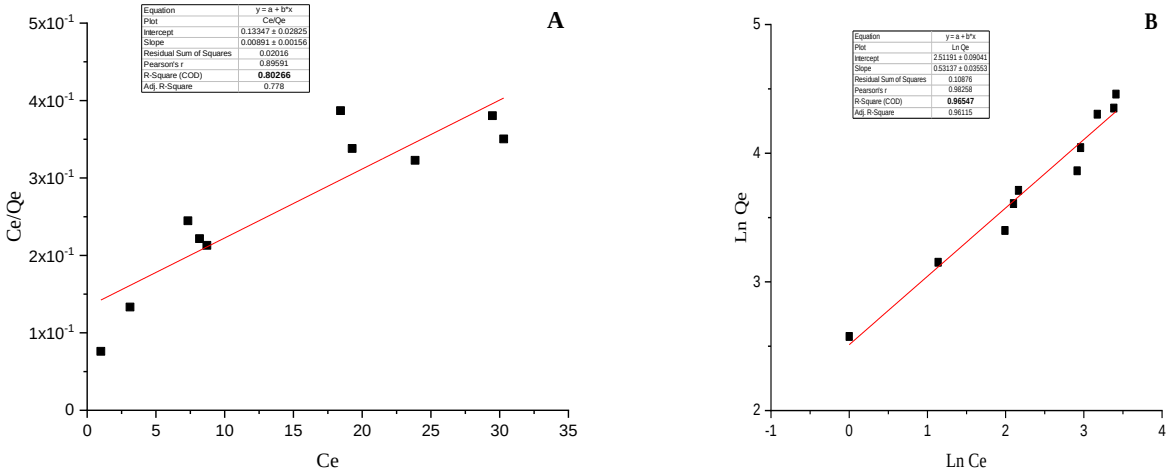

Figure 9. Plots of (A) Langmuir model and (B) Freundlich model

Table 3. ***Langmuir and Freundlich isotherm parameters***

Langmuir model			**Freundlich model**		
K_L	q_{max}	R^2	K_F	1/n	R^2
($L.mg^{-1}$)	($mg.g^{-1}$)		($mg.g^{-1}$) ($L.mg^{-1}$)$^{-1/n}$		
0.067	112.36	0.8027	12.32	0.53	0.965

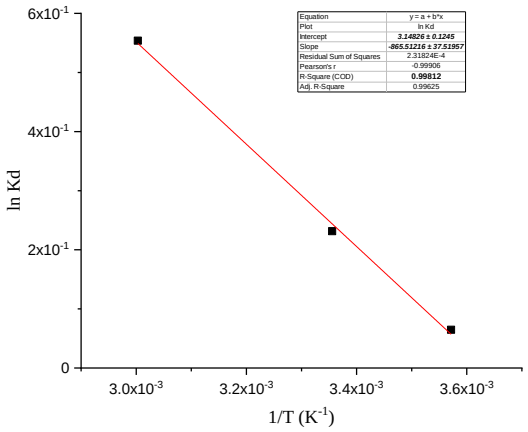

Figure 10. Linear plot of ln (K) versus (1/T) for the adsorption of BET dye onto the adsorbent

3.5. Thermodynamic study

The observed increase in the capacity adsorption of dye on adsorbent with the increase in temperature is indicative of the fact that the adsorption process is endothermic in nature. ***Figure 10*** presents the plot of linear transform of Ln (K) versus (1 / T)

Table 4: ***Thermodynamic parameters***

Temperature (°K)	**ΔH° (kJ.mol^{-1})**	**ΔS° (J.mol^{-1}.K^{-1})**	**ΔG° (J.mol^{-1})**	**R²**
280	7.2	26.2	-133.1	0.998
298			-604.3	
333			-1520.4	

Thermodynamic study

The observed increase in the capacity adsorption of dye on adsorbent with the increase in temperature is indicative of the fact that the adsorption process is endothermic in nature. ***Figure 10*** presents the plot of linear transform of Ln (K) versus (1 / T)

Table 4 shows the results obtained for the thermodynamic adsorption parameters. The positive value of the enthalpy ΔH° indicates that the adsorption process of NET on CaPT-Ap is endothermic in nature (by increasing T we promote adsorption) [47]. The positive value of the entropy ΔS° means that the adsorption is accompanied by a disorder of the medium thus showing that the molecules of the dye adsorbed on the surface of the adsorbent are organized randomly. Likewise, the negative values of the Gibbs free energy ΔG ° at each temperature, confirm that the adsorption of the dye on the surface of the adsorbent is a spontaneous process [48][49].

4. Conclusion

Generally, the method used to prepare the CaPT-Ap was efficient and successful, as shown by the characterization analysis. In the present work, we tested the adsorption of EBT on CaPT-Ap prepared by co-precipitation at ambient temperature in a basic medium. The results show that the adsorption kinetic of EBT is well described by the pseudo-second-order model. The adsorptions isotherms satisfactorily by the Freundlich model and the thermodynamic study indicates that the adsorption process is a spontaneous, disordered and endothermic physisorption.

All characteristics indicate that CaPT-Ap could be used as an efficient and low-cost adsorbent for water treatment.

References

[1]M. T. Yagub, T. K. Sen, S. Afroze, and H. M. Ang, “Dye and its removal from aqueous solution by adsorption: A review,” *Adv. Colloid Interface Sci.*, vol. 209, pp. 172–184, 2014, doi: 10.1016/j.cis.2014.04.002.

[2]C. Tcheka, D. Abia, D. Iya-sou, and A. L. T. Tamgue, “Removal Of Crystal Violet Dye From Aqueous Solutions Using Chemically Activated Carbons By H3po4 Activation From Corn Cobs And Corn Roots: Kinetic And Equilibrium Isotherm Studies,” *Moroccan J. Chem.*, vol. 9, no. 2, pp. 221–231, 2021, doi:

10.48317/IMIST.PRSM/MORJCHEM-V9I2.22099.
[3]N. Hassan, A. Shahat, A. El-Didamony, M. G. El-Desouky, and A. A. El-Bindary, “Equilibrium, Kinetic and Thermodynamic studies of adsorption of cationic dyes from aqueous solution using ZIF-8,” *Moroccan J. Chem.*, vol. 8, no. 3, pp. 624–635, 2020, doi: 10.48317/IMIST.PRSM/morjchem-v8i3.21127.
[4]S. V. Dorozhkin, “Calcium orthophosphates in nature, biology and medicine,” *Materials*, vol. 2, no. 2. pp. 399–498, 2009, doi: 10.3390/ma2020399.
[5]G. Penel, G. Leroy, C. Rey, and E. Bres, “MicroRaman spectral study of the PO 4 and CO 3 vibrational modes in synthetic and biological apatites,” *Calcif. Tissue Int.*, vol. 63, no. 6, pp. 475–481, 1998.
[6]A. Ogose *et al.*, “Comparison of hydroxyapatite and beta tricalcium phosphate as bone substitutes after excision of bone tumors,” *J. Biomed. Mater. Res. - Part B Appl. Biomater.*, 2005, doi: 10.1002/jbm.b.30136.
[7]P. A. F. Sossa, B. S. Giraldo, B. C. G. Garcia, E. R. Parra, and P. J. A. Arango, “Comparative study between natural and synthetic hydroxyapatite: Structural, morphological and bioactivity properties,” *Rev. Mater.*, vol. 23, no. 4, 2018, doi: 10.1590/s1517-707620180004.0551.
[8]D. Tadic, “A thorough physicochemical characterisation of 14 calcium phosphate-based bone substitution materials in comparison to natural bone,” *Biomaterials*, 2003, doi: 10.1016/s0142-9612(03)00621-5.
[9]A. Antonakos, E. Liarokapis, and T. Leventouri, “Micro-Raman and FTIR studies of synthetic and natural apatites,” *Biomaterials*, vol. 28, no. 19, pp. 3043–3054, 2007.
[10] F. B. H. Yahia and M. Jemal, “Synthesis, structural analysis and thermochemistry of B-type carbonate apatites,” *Thermochim. Acta*, vol. 505, no. 1–2, pp. 22–32, 2010.
[11] I. Cacciotti, A. Bianco, M. Lombardi, and L. Montanaro, “Mg-substituted hydroxyapatite nanopowders: Synthesis, thermal stability and sintering behaviour,” *J. Eur. Ceram. Soc.*, 2009, doi: 10.1016/j.jeurceramsoc.2009.04.038.
[12] N. Y. Mostafa, H. M. Hassan, and F. H. Mohamed, “Sintering behavior and thermal stability of Na+, SiO44− and CO32− co-substituted hydroxyapatites,” *J. Alloys Compd.*, vol. 479, no. 1, pp. 692–698, 2009, doi: https://doi.org/10.1016/j.jallcom.2009.01.037.
[13] A. Elouahli *et al.*, “Apatitic tricalcium phosphate powder: High sorption capacity of hexavalent chromium removal,” *Surfaces and Interfaces*, vol. 13, no. September, pp. 139–147, 2018, doi: 10.1016/j.surfin.2018.09.006.
[14] I. Mobasherpour, E. Salahi, and M. Pazouki, “Removal of nickel (II) from aqueous solutions by using nano-crystalline calcium hydroxyapatite,” *J. Saudi Chem. Soc.*, vol. 15, no. 2, pp. 105–112, 2011.
[15] H. El Boujaady, A. El Rhilassi, M. Bennani-ziatni, R. El Hamri, A. Taitai, and J. L. Lacout, “Removal of a textile dye by adsorption on synthetic calcium phosphates,” *DES*, vol. 275, no. 1–3, pp. 10–16, 2011, doi: 10.1016/j.desal.2011.03.036.
[16] F. S. Souza, M. J. S. Matos, B. R. L. Galvão, A. F. C. Arapiraca, S. N. da Silva, and I. P. Pinheiro, “Adsorption of CO2 on biphasic and amorphous calcium phosphates: An experimental and theoretical analysis,” *Chem. Phys. Lett.*, 2019, doi: 10.1016/j.cplett.2018.10.080.
[17] K. Ohta, H. Monma, and S. Takahashi, “Adsorption characteristics of proteins on calcium phosphates using liquid chromatography,” *J. Biomed. Mater. Res.*, 2001, doi: 10.1002/1097-4636(20010605)55:3<409::AID-JBM1030>3.0.CO;2-Z.
[18] M. A. Spinelli, F. Brudevold, and E. Moreno, “Mechanism of fluoride uptake by hydroxyapatite,” *Arch. Oral Biol.*, 1971, doi: 10.1016/0003-9969(71)90106-3.
[19] N. H. De Leeuw, “A computer modelling study of the uptake and segregation of fluoride ions at the

hydrated hydroxyapatite (0001) surface: Introducing a Ca10(PO4)6(OH)2potential model," 2004, doi: 10.1039/b313242k.
[20] M. Mourabet, A. El Rhilassi, M. Bennani-Ziatni, R. El Hamri, and A. Taitai, "Studies on fluoride adsorption by apatitic tricalcium phosphate (ATCP) from aqueous solution," *Desalin. Water Treat.*, vol. 51, no. 34–36, pp. 6743–6754, 2013, doi: 10.1080/19443994.2013.769728.
[21] M. Mourabet, A. El Rhilassi, H. El Boujaady, M. Bennani-Ziatni, R. El Hamri, and A. Taitai, "Removal of fluoride from aqueous solution by adsorption on hydroxyapatite (HAp) using response surface methodology," *J. Saudi Chem. Soc.*, vol. 19, no. 6, pp. 603–615, 2015, doi: 10.1016/j.jscs.2012.03.003.
[22] S. Fan *et al.*, "Magnetic chitosan-hydroxyapatite composite microspheres: Preparation, characterization, and application for the adsorption of phenolic substances," *Bioresour. Technol.*, vol. 274, pp. 48–55, 2019, doi: https://doi.org/10.1016/j.biortech.2018.11.078.
[23] S. Ravi, Y. Choi, and J. K. Choe, "Novel phenyl-phosphate-based porous organic polymers for removal of pharmaceutical contaminants in water," *Chem. Eng. J.*, vol. 379, p. 122290, Jan. 2020, doi: 10.1016/j.cej.2019.122290.
[24] E. H. Mourid, I. El Qor, L. Benaziz, M. Lakraimi, and E. H. El Khattabi, "Evaluation of the adsorption capacity of Natural Phosphate to remove Remazol Brilliant Blue R dye in aqueous solution," *Moroccan J. Chem.*, vol. 6, no. 3, pp. 425–433, 2018, doi: 10.48317/IMIST.PRSM/MORJCHEM-V6I3.11110.
[25] J.-C. Heughebaert and G. Montel, "Conversion of amorphous tricalcium phosphate into apatitic tricalcium phosphate.," *Calcif. Tissue Int.*, vol. 34, pp. S103-8, 1982.
[26] J. C. Heughebaert, "Contributiona l'Étude de l'Évolution des Orthophosphates de Calcium Précipités en Orthophosphates Apatitiques," *Inst. Natl. Polytech. Toulouse, Toulouse, Fr.*, 1977.
[27] J.-C. Heughebaert and G. Montel, "Étude de l'évolution de l'orthophosphate tricalcique non cristallin en phosphate apatitique à la faveur d'une réaction chimique, à température ordinaire," *Rev. Phys. Appliquée*, vol. 12, no. 5, pp. 691–694, 1977.
[28] Y. S. Ho and G. Mckay, "Kinetic Models for the Sorption of Dye from Aqueous Solution by Wood," *Process Saf. Environ. Prot.*, vol. 76, no. 2, pp. 183–191, May 1998, doi: 10.1205/095758298529326.
[29] I. Langmuir, "The constitution and fundamental properties of solids and liquids. Part I. Solids.," *J. Am. Chem. Soc.*, vol. 38, no. 11, pp. 2221–2295, 1916.
[30] H. M. F. Freundlich, "Over the adsorption in solution," *J. Phys. Chem*, vol. 57, no. 385471, pp. 1100–1107, 1906.
[31] N. A. Jarrah, "Adsorption of Cu (II) and Pb (II) from aqueous solution using Jordanian natural zeolite based on factorial design methodology," *Desalin. Water Treat.*, vol. 16, no. 1–3, pp. 320–328, 2010.
[32] M. N. Sepehr, T. J. Al-Musawi, E. Ghahramani, H. Kazemian, and M. Zarrabi, "Adsorption performance of magnesium/aluminum layered double hydroxide nanoparticles for metronidazole from aqueous solution," *Arab. J. Chem.*, vol. 10, no. 5, pp. 611–623, 2017.
[33] M. Kawata, H. Uchida, K. Itatani, I. Okada, S. Koda, and M. Aizawa, "Development of porous ceramics with well-controlled porosities and pore sizes from apatite fibers and their evaluations," *J. Mater. Sci. Mater. Med.*, vol. 15, no. 7, pp. 817–823, 2004.
[34] B. Nasiri-Tabrizi, A. Fahami, and R. Ebrahimi-Kahrizsangi, "Effect of milling parameters on the formation of nanocrystalline hydroxyapatite using different raw materials," *Ceram. Int.*, vol. 39, no. 5, pp. 5751–5763, 2013.

[35] F. Bakan, O. Laçin, and H. Sarac, “A novel low temperature sol–gel synthesis process for thermally stable nano crystalline hydroxyapatite,” *Powder Technol.*, vol. 233, pp. 295–302, 2013.
[36] H. K. Varma and S. S. Babu, “Synthesis of calcium phosphate bioceramics by citrate gel pyrolysis method,” *Ceram. Int.*, vol. 31, no. 1, pp. 109–114, 2005.
[37] J. C. P. Vaghetti *et al.*, “Application of Brazilian-pine fruit coat as a biosorbent to removal of Cr (VI) from aqueous solution—Kinetics and equilibrium study,” *Biochem. Eng. J.*, vol. 42, no. 1, pp. 67–76, 2008.
[38] B. C. Smith, *Infrared spectral interpretation: a systematic approach*. CRC press, 2018.
[39] T. Calvete, E. C. Lima, N. F. Cardoso, J. C. P. Vaghetti, S. L. P. Dias, and F. A. Pavan, “Application of carbon adsorbents prepared from Brazilian-pine fruit shell for the removal of reactive orange 16 from aqueous solution: Kinetic, equilibrium, and thermodynamic studies,” *J. Environ. Manage.*, vol. 91, no. 8, pp. 1695–1706, 2010.
[40] A. C. Chapman and L. E. Thirlwell, “Spectra of phosphorus compounds—I the infra-red spectra of orthophosphates,” *Spectrochim. Acta*, vol. 20, no. 6, pp. 937–947, 1964.
[41] B. O. Fowler, E. C. Moreno, and W. E. Brown, “Infra-red spectra of hydroxyapatite, octacalcium phosphate and pyrolysed octacalcium phosphate,” *Arch. Oral Biol.*, vol. 11, no. 5, pp. 477–492, 1966.
[42] H. El Boujaady, M. Mourabet, A. El Rhilassi, M. Bennani-Ziatni, R. El Hamri, and A. Taitai, “Interaction of adsorption of reactive yellow 4 from aqueous solutions onto synthesized calcium phosphate,” *J. Saudi Chem. Soc.*, vol. 21, pp. S94–S100, 2017, doi: 10.1016/j.jscs.2013.10.009.
[43] C. Combes and C. Rey, “Amorphous calcium phosphates: Synthesis, properties and uses in biomaterials,” *Acta Biomaterialia*. 2010, doi: 10.1016/j.actbio.2010.02.017.
[44] S. D. E. Nanoparticules *et al.*, “VOIE AQUEUSE β -TCP were synthesized by wet precipitation method in aqueous phase . The size of the crystallites is closed to 40 nm . The two powders , dried at 60 ° C and calcined at 800 ° C were characterized by using X-ray diffraction (XRD), infrared,” vol. 4, pp. 1–6, 2015.
[45] B. Nasiri-Tabrizi and A. Fahami, “Mechanochemical synthesis and structural characterization of nano-sized amorphous tricalcium phosphate,” *Ceram. Int.*, 2013, doi: 10.1016/j.ceramint.2013.04.045.
[46] K. Allam, A. El Bouari, B. Belhorma, and L. Bih, “Removal of Methylene Blue from Water Using Hydroxyapatite Submitted to Microwave Irradiation,” *J. Water Resour. Prot.*, vol. 08, no. 03, pp. 358–371, 2016, doi: 10.4236/jwarp.2016.83030.
[47] Y. Dehmani, O. El Khalki, H. Mezougane, and S. Abouarnadasse, “Comparative study on adsorption of cationic dyes and phenol by natural clays,” *Chem. Data Collect.*, vol. 33, p. 100674, 2021, doi: 10.1016/j.cdc.2021.100674.
[48] T. C. Egbosiuba *et al.*, “Adsorption of Cr(VI), Ni(II), Fe(II) and Cd(II) ions by KIAgNPs decorated MWCNTs in a batch and fixed bed process,” *Sci. Rep.*, vol. 11, no. 1, pp. 1–20, 2021, doi: 10.1038/s41598-020-79857-z.
[49] N. Danesh, M. Ghorbani, and A. Marjani, “Separation of copper ions by nanocomposites using adsorption process,” *Sci. Rep.*, vol. 11, no. 1, pp. 1–23, 2021, doi: 10.1038/s41598-020-80914-w.